nature structural & molecular biology

Structural basis for recruitment of GRIP domain golgin-245 by small GTPase Arl1

Mousheng Wu[1,3,4], Lei Lu[2,4], Wanjin Hong[2] & Haiwei Song[1,3]

Recruitment of the GRIP domain golgins to the *trans*-Golgi network is mediated by Arl1, a member of the ARF/Arl small GTPase family, through interaction between their GRIP domains and Arl1-GTP. The crystal structure of Arl1-GTP in complex with the GRIP domain of golgin-245 shows that Arl1-GTP interacts with the GRIP domain predominantly in a hydrophobic manner, with the switch II region conferring the main recognition surface. The involvement of the switch and interswitch regions in the interaction between Arl1-GTP and GRIP accounts for the specificity of GRIP domain for Arl1-GTP. Mutations that abolished the Arl1-mediated Golgi localization of GRIP domain golgins have been mapped on the interface between Arl1-GTP and GRIP. Notably, the GRIP domain forms a homodimer in which each subunit interacts separately with one Arl1-GTP. Mutations disrupting the GRIP domain dimerization also abrogated its Golgi targeting, suggesting that the dimeric form of GRIP domain is a functional unit.

Protein trafficking along secretory and endocytic pathways is regulated by members of the Ras-like small GTPase superfamily[1,2]. Members of ARF/Arl family small GTPases, such as Sar1, ARF1–6 and Arl1, contribute to membrane trafficking at multiple stages of exocytic and endocytic pathways. Arls are ~40–60% identical to each other and to ARFs[3–5]. Recent studies on Arls suggest that they have diverse functions in multiple organelles, including regulation of Golgi structure and functions by Arl1 (refs. 4,6,7), regulation of microtubule network dynamics by Arl2 and Arl3 (refs. 8–13), mitochondria transport by Arl2 (ref. 14), endoplasmic reticulum (ER) protein translocation by Arl6 (ref. 15) and nuclear dynamics and signaling by Arl4, Arl4L and Arl7 (refs. 5,16–20).

Arl1 is the only member of the Arl subfamily that has been shown to be Golgi-associated, thereby regulating the structure and function of the Golgi apparatus[6,7]. Several putative effectors of Arl1 have been identified by yeast two-hybrid screening, including POR1, pericentrin, golgin-245 and golgin-97. Golgin-245, golgin-97, GCC88 and GCC185 form a unique subfamily of golgins containing a conserved GRIP domain at the C terminus[21–24]. Golgins are a family of Golgi-localized proteins with extensive coiled-coil regions that have been proposed to adopt rodlike structures and serve as Golgi matrix and vesicle tethering molecules[25]. All known golgins are anchored to the Golgi membrane by their extreme C termini. The GRIP domains found in golgin-97, golgin-245/p230, GCC88 and GCC185 are evolutionarily conserved, and are necessary and sufficient for the Golgi localization of golgins via a saturable mechanism[21–24,26,27]. Three recent studies (two in yeast and one in mammalian cells) have shown that golgins containing GRIP domain are effectors of Arl1, and that Arl1-GTP recruits these golgins to the Golgi membrane by interacting with their GRIP domains[28–31]. The interaction is dependent on conserved residues of the GRIP domain and the switch II region of Arl1 (ref. 28).

To investigate how Arl1-GTP and GRIP domain interact and function in Golgi targeting, we have determined the crystal structure of Arl1-GTP in complex with the GRIP domain of golgin-245/p230 at a resolution of 2.3 Å. The structure reveals that the GRIP domain forms a homodimer in which each subunit interacts with one Arl1-GTP. By comparison with the GDP-bound form of Arl1, the structure accounts for why only Arl1-GTP and not Arl1-GDP binds to the GRIP domain. Mutagenesis combined with structural data suggest that the dimeric form of GRIP domain is a structural and functional unit in Golgi targeting. The structure provides a framework for the molecular mechanism underlying Golgi recruitment of GRIP domain golgins by Arl1-GTP.

RESULTS

Structural overview of the Arl1–GRIP complex

The crystal structure of a complex (designated as Arl1–GRIP) formed by the GRIP domain (residues 2171–2230) of human golgin-245 and rat Arl1 (lacking the 14 N-terminal residues) with bound GDPNP was determined at a resolution of 2.3 Å (see Methods and **Table 1**). A representative portion of the initial electron density map in the region of GRIP domain is shown in **Figure 1a**. The final model includes most of the GRIP domain and Arl1 amino acids with the exception of a C-terminal segment (residues 2223–2230) of GRIP domain.

[1]Laboratory of Macromolecular Structure, Institute of Molecular and Cell Biology, 30 Medical Drive, Singapore 117609. [2]Laboratory of Membrane Biology, Institute of Molecular and Cell Biology, 30 Medical Drive, Singapore 117609. [3]Department of Biological Sciences, National University of Singapore, 14 Science Drive 4, Singapore 117543. [4]These authors contributed equally to this work. Correspondence should be addressed to W.H. (mcbhwj@imcb.a-star.edu.sg) or H.S. (haiwei@imcb.a-star.edu.sg).

Published online 29 December 2003; doi:10.1038/nsmb714

GRIP domain forms a tight homodimer in which each subunit binds to one Arl1-GTP on opposite sides, thus forming a heterodimeric dimer composed of two GRIP domains and two Arl1-GTP molecules, which can be best described as Arl1–$(GRIP)_2$–Arl1 rather than $(Arl1–GRIP)_2$ or $(Arl1)_2$–$GRIP_2$ (**Fig. 1b,c**). The other heterodimeric dimer in the asymmetric unit is related by a two-fold noncrystallographic symmetry operation. These observations are in agreement with our gel filtration results, in which the Arl1–GRIP complex was eluted with a Arl1/GRIP molar ratio of 2:2 (data not shown). Arl1-GTP in the Arl1–GRIP complex shows the typical G domain fold of Ras-like small GTPases with a six-stranded β-sheet surrounded by five α-helices. The conformational changes of switch regions induced by GDPNP binding resemble closely those observed in other small GTPases upon GTP binding[32]. The GRIP domain folds into three anti-parallel α-helices arranged in a twisted array rather than a three-helix bundle; one side of the array is used for dimerization and the other to interact with Arl1-GTP. The homodimer of GRIP domains forms a six-helix bundle in a parallel fashion, interacting with the NCS-related homodimer in a head-to-tail manner. There are very few interactions between Arl1 molecules. In contrast, GRIP domains interact extensively in the homodimer interface.

Arl1–GRIP domain interface

The structure shows that Arl1-GTP and GRIP domain share an extensive interface. The interaction between Arl1-GTP and GRIP domain buries a pairwise accessible surface area of 1,272 Å^2. GRIP domain interacts with Arl1-GTP via its first two helices, α1 and α2. Arl1-GTP interacts with GRIP domain mainly through its switch II region, with additional residues from the switch I and interswitch regions (**Fig. 2a**). These observations are consistent with earlier studies showing that the switch II region of Arl1 confers the specificity of its interaction with the GRIP domain[28]. The recognition specificity between Arl1-GTP and GRIP domain is achieved predominantly through hydrophobic interactions, with two additional hydrogen bonds (**Fig. 2a**). The surface groove on Arl1-GTP that interacts with the GRIP domain is composed mainly of hydrophobic amino acids (Ile49, Phe51, Gln64, Trp66, Gln71, Ser73, Ile74, Tyr77, Cys80 and Tyr81). These residues are in the switch and interswitch regions and most of them are highly conserved in Arls or ARFs, except for residues Ile49, Ser73 and Cys80 (**Fig. 3a**). Cys80 is present only in Arl1 and not other Arls or ARFs. Mutation of Cys80, which is highly conserved in all Arl1 from various species, to histidine substantially reduced the ability of Arl1 to interact with the GRIP domain of golgin-245 (ref. 28), suggesting that Cys80 may have an important role in the interactions of Arl1-GTP with the GRIP domain. Cys80 is situated at the edge of the hydrophobic interface and makes a hydrophobic interaction with Val2197 of GRIP domain (**Fig. 2a**). Replacement of this residue with a large polar amino acid such as histidine may cause steric hindrance and/or destabilization of the hydrophobic interface, thus weakening the binding of Arl1-GTP to GRIP.

The surface area of GRIP domain that interacts with Arl1-GTP consists of hydro-

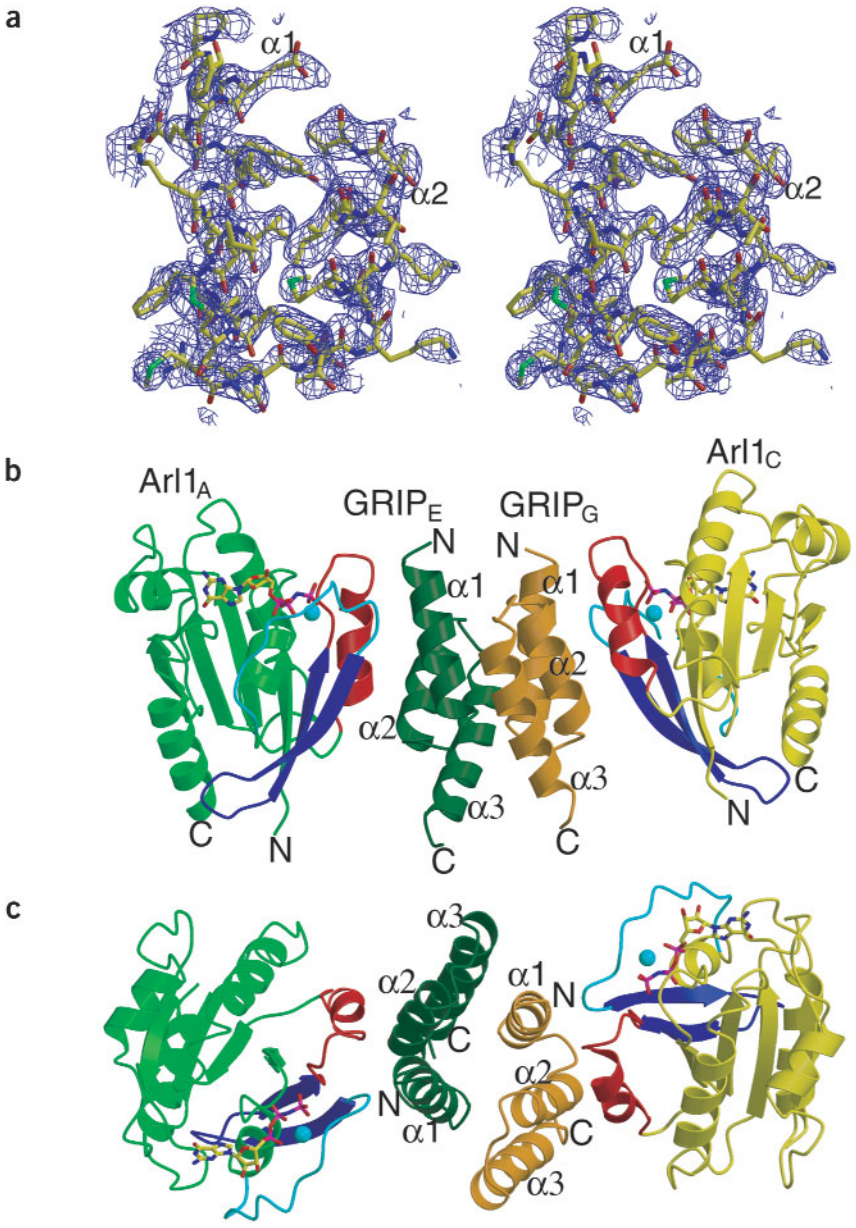

Figure 1 Structure of the Arl1–GRIP complex. (**a**) Stereo view of a representative portion of the $F_o - F_c$ electron density map (contoured at 1.2 σ) covering helices α1 and α2 of the GRIP domain. The map was calculated with phases from Arl1 molecules only. The percentages of scattering matter contributed by the GRIP domain and the Arl1 molecule are 28% and 72%, respectively. (**b**) The Arl1–GRIP heterodimeric dimer formed by Arl1 molecules A (green) and C (yellow), and the GRIP domains E (dark green) and G (orange). Switch I, interswitch and switch II of Arl1 are cyan, blue and red, respectively. GDPNP molecules are shown in stick model and Mg^{2+} as cyan spheres. (**c**) Top view of the Arl1–GRIP heterodimeric dimer. The molecules are rotated 90° relative to the view in **b**.

phobic residues Tyr2177, Val2181, Met2194, Val2197 and Val2201, and the additional polar and charged residues Thr2173, Glu2174, Glu2176 and Thr2193 (**Fig. 2a**). Most of these residues are conserved in GRIP domains across species (**Fig. 3b**). Close inspection of the structure shows that Tyr2177, the only invariant aromatic residue in GRIP domain, makes extensive hydrophobic interactions with residues in the switch II region of Arl1. The side chain of Tyr2177 fits tightly into a hydrophobic pocket formed by the side chains of Ile74, Tyr77, Cys80 and Tyr81 in the switch II region in Arl1. In addition to the hydrophobic interactions, the hydroxyl group of Tyr2177 is hydrogen bonded to that of Tyr81 of the switch II region in Arl1. These interactions suggest that replacement of Tyr2177 by any other nonaromatic residue would reduce the binding of GRIP to Arl1 substantially. This observation accounts for the finding that a Y2177A mutation in the GRIP domain of golgin-245 abolished its Golgi targeting (mediated by the interactions between Arl1-GTP and its GRIP domain), whereas a Y2177F mutation had little effect[22,23]. Similar results have been obtained for a Y697A mutation in golgin-97 (counterpart of Tyr2177 of golgin-245)[28]. In addition to contacts with Tyr2177, the switch II region also interacts with residues in helix α2 of GRIP (**Fig. 2a**). Tyr77 interacts with Val2201 while Cys80 and Tyr81 make multiple hydrophobic and van der Waals interactions with the side chains of Val2197 and Thr2193. The hydroxyl group of Tyr77 makes a hydrogen bond with the OE1 atom of Glu2174 in GRIP domain. The extensive interactions contributed by the switch II region to the Arl1–GRIP interface suggest that the switch II region may have an indispensable role in GRIP domain recognition. Consistent with these observations, replacement of the whole switch II region of Arl1 with corresponding ARF1 residues completely abolished the interaction of Arl1-GTP with the GRIP domain[28]. Additional contacts in the Arl1–GRIP interface are made among residues in the switch I and interswitch regions and residues in helix α1 of the GRIP domain (**Fig. 2a**). Specifically, the side chain of Ile49 of the switch I region interacts with that of Glu2176. In the interswitch region, Phe51 makes a strong hydrophobic interaction with Met2194 and a van der Waals interaction with Glu2184; both Gln64 and Trp66 make hydrophobic and van der Waals interactions with Glu2190. We conducted structure-guided mutagenesis to study the roles of residues involved in interactions between Arl1-GTP and the GRIP domain related to Golgi targeting. V2181A, T2193A, M2194A and V2197A mutations in the GRIP domain of golgin-245 abolished its Golgi targeting (**Fig. 4a,c**). These observations combined with earlier mutational studies of Tyr2177 (refs. 22,27,28) suggest that the specific interactions between Arl1 and GRIP domain are essential for Golgi localization of the GRIP domain golgins.

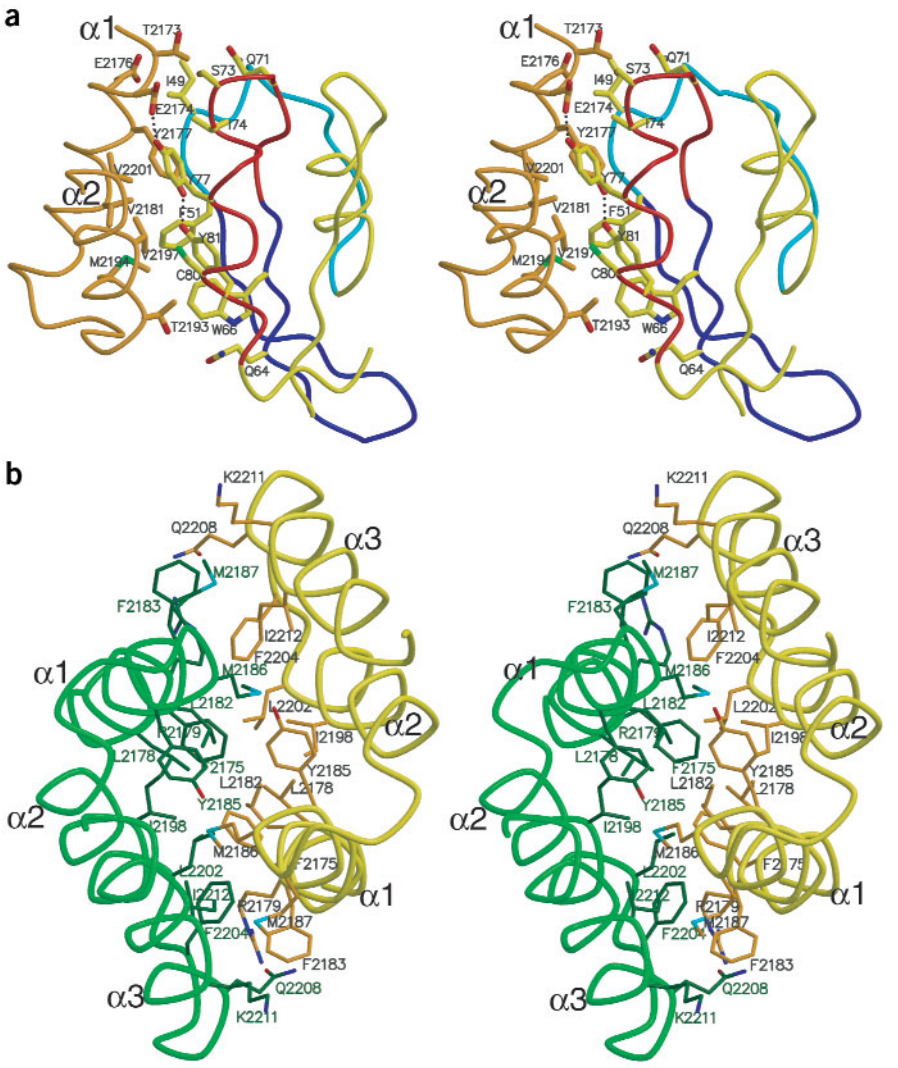

Figure 2 Arl1–GRIP and GRIP–GRIP interfaces. (**a**) Stereo diagram of the Arl1–GRIP interface. The GRIP domain (chain E) is orange and the Arl1 molecule (chain A) yellow. Switch I, switch II and interswitch regions of Arl1 are cyan, red and blue, respectively, and the rest of Arl1 is yellow. Residues involved in Arl1–GRIP interactions are shown in stick models. Hydrogen bonds are black dashed lines. (**b**) Stereo diagram of the GRIP–GRIP interface. The GRIP domains of chain E and G are green and yellow, respectively. Residues involved in GRIP–GRIP interactions are shown in stick models and labeled in dark green and brown for chains E and G, respectively.

GRIP–GRIP domain interface

The structure shows that GRIP domains form a tight homodimer. There are two homodimers (E–G and H–F) of GRIP domains in the asymmetric unit. Because the E–G dimer is very similar to the H–F dimer (with pairwise r.m.s. deviation of 0.2 Å), we chose the E–G dimer (**Fig. 1b**) to illustrate the GRIP–GRIP interface. The interactions in the E–G dimer interface are predominantly hydrophobic with a buried accessible surface area of 1,880 Å^2. All three α-helices of GRIP domain are involved in dimerization.

The surface area of the GRIP domain involved in dimerization is composed of four aromatic amino acids (Phe2175, Phe2183, Tyr2185 and Phe2204), seven hydrophobic residues (Leu2178, Leu2182, Met2186, Met2187, Ile2198, Leu2202 and Ile2212), two charged residues (Arg2179 and Lys2211) and one polar residue (Gln2208). These residues in GRIP$_E$ make multiple van der Waals and hydrophobic interactions with the same set of residues in GRIP$_G$

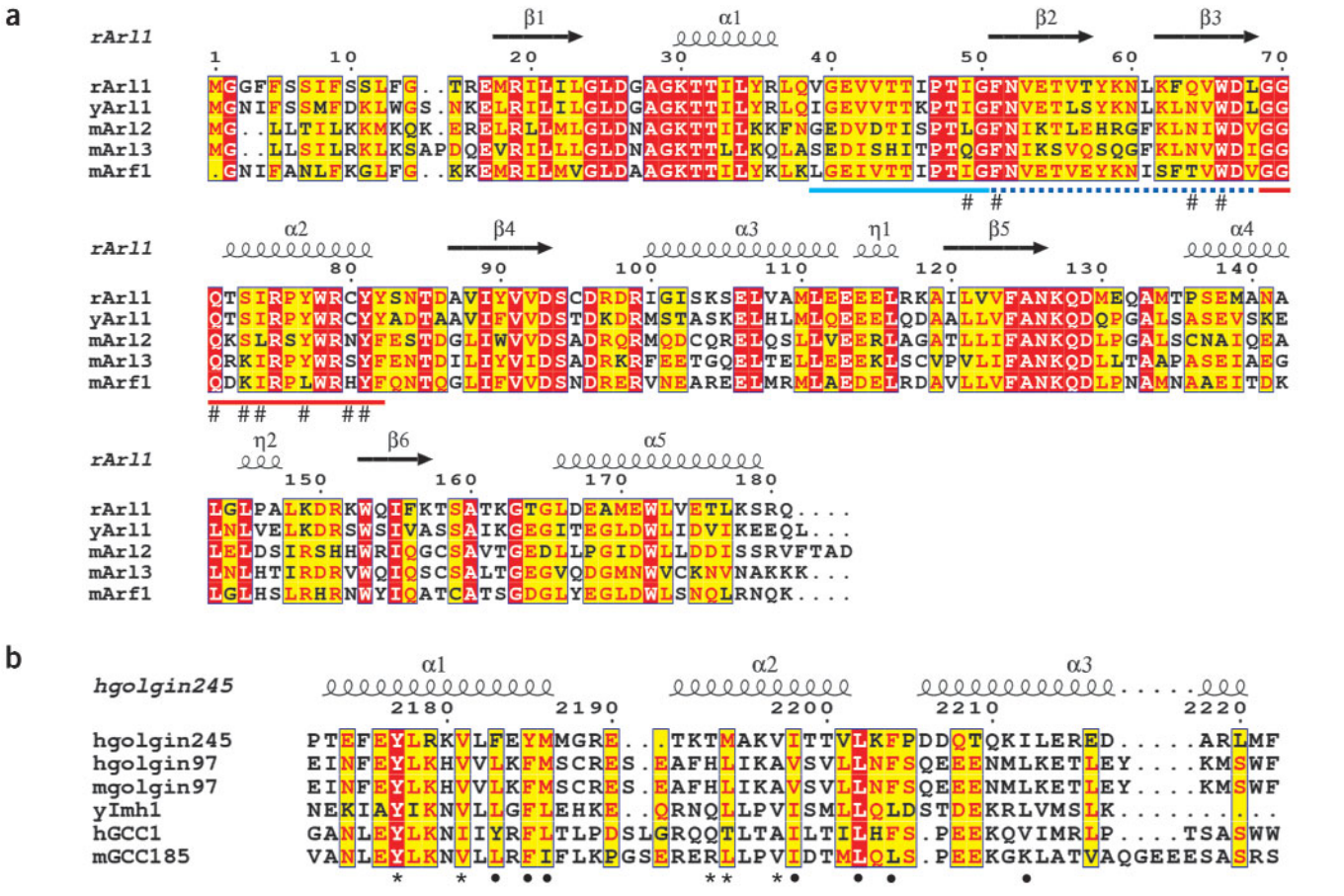

Figure 3 Sequence alignment of Arls and GRIP domains. (**a**) Alignment of amino acid sequences of rat Arl1, *S. cerevisiae* Arl1 and mouse Arl2, Arl3 and ARF1. Secondary structures for rat Arl1 are at top. The switch I, II and interswitch regions are marked with cyan, red and blue (dashed) lines, respectively. #, residues involved in interactions with the GRIP domains. Invariant residues are white letters, similar residues are red and others are black. Residues with similarity between 0.7 and 1.0 as defined in ENDscript[50] are boxed in blue. (**b**) Alignment of the conserved GRIP domain of human golgin-245, human golgin-97, mouse golgin-97, *S. cerevisiae* Imh1p, human GCC1 (GCC88) and mouse GCC185. The secondary structures of the GRIP domain of human golgin-245 are shown. Mutated residues involved in GRIP domain dimerization and interactions with Arl1-GTP are marked • and ∗, respectively. The coloring scheme is as in **a**.

(subscripted E and G designate the E and G chains of the of GRIP domain, respectively).

In the dimer interface (**Fig. 2b**), beginning from the N terminal of helix α1, Phe2175$_E$ makes strong hydrophobic interactions with its two-fold NCS-related counterpart Phe2175$_G$. Arg2179$_E$, a conserved residue in GRIP domain, interacts with Leu2202$_G$ and Phe2204$_G$ via hydrophobic interactions, with its methylene group stacking against the aromatic ring of Phe2204$_G$. In support of this observation, a K699A mutation (corresponding to Arg2179 of golgin-245) in golgin-97 abrogated the Golgi targeting of the mutant protein[28], underscoring the importance of this residue in GRIP dimerization. Leu2182$_E$ contacts Leu2202$_G$ and Phe2204$_G$, respectively, whereas Phe2183$_E$ interacts with Leu2212$_G$ and the aliphatic side chain of Gln2208$_G$. A conserved Tyr2185$_E$ makes strong hydrophobic interactions with its two-fold NCS-related counterpart Tyr2185$_G$ and with Met2186$_G$, suggesting that this residue may have an important role in dimerization. Met2186$_E$ and Met2187$_E$ make multiple van der Waals and hydrophobic interactions with Tyr2185$_G$, Ile2198$_G$, Ile2212$_G$ and Lys2211$_G$. Ile2198$_E$ of helix α2 makes van der Waals interactions with Met2186$_G$ whereas Leu2202$_E$, the second invariant residue in GRIP domain across species, makes a strong hydrophobic interaction with Leu2182$_G$. In addition to the intermolecular interactions, Leu2202$_E$ makes close intramolecular contacts with Phe2204$_E$, which in turn makes stacking interactions between its aromatic ring and the aliphatic side chain of Arg2179$_G$. The methylene group of Lys2211$_E$ of helix α3 packs against the side chain of Met2187$_G$. Ile2212$_E$ is situated in the middle of α3, making multiple contacts with Phe2183$_G$, Met2186$_G$ and Met2187$_G$.

The extensive dimer interface and the involvement of some highly conserved residues in GRIP domain suggest that the homodimer of GRIP domains may function as a structural unit for interaction with Arl1 to mediate Golgi localization of golgin-245. A Y2185A mutation in golgin-245 has been shown to abolish Golgi targeting of the mutant protein[22], but the mechanism of how Tyr2185 affects Golgi targeting is not yet known. Our observations suggest that the Y2185A mutation may disrupt the GRIP dimerization, hence affecting the Golgi localization of golgin-245. We mutated additional residues involved in the GRIP-GRIP interactions to study their effects on Golgi targeting. As predicted, golgin-245 point mutants F2183A, M2186A, I2198A, L2202A, F2204A and I2212A were not Golgi-associated (**Fig. 4a**,**c**). Phe2183, Tyr2185, Met2186, Ile2198, Leu2202, Phe2204 and Ile2212 make no direct contacts with Arl1-GTP, but substitutions of these residues with alanine still abolished the Golgi targeting of golgin-245. One likely explanation for this observation is that mutations disrupt-

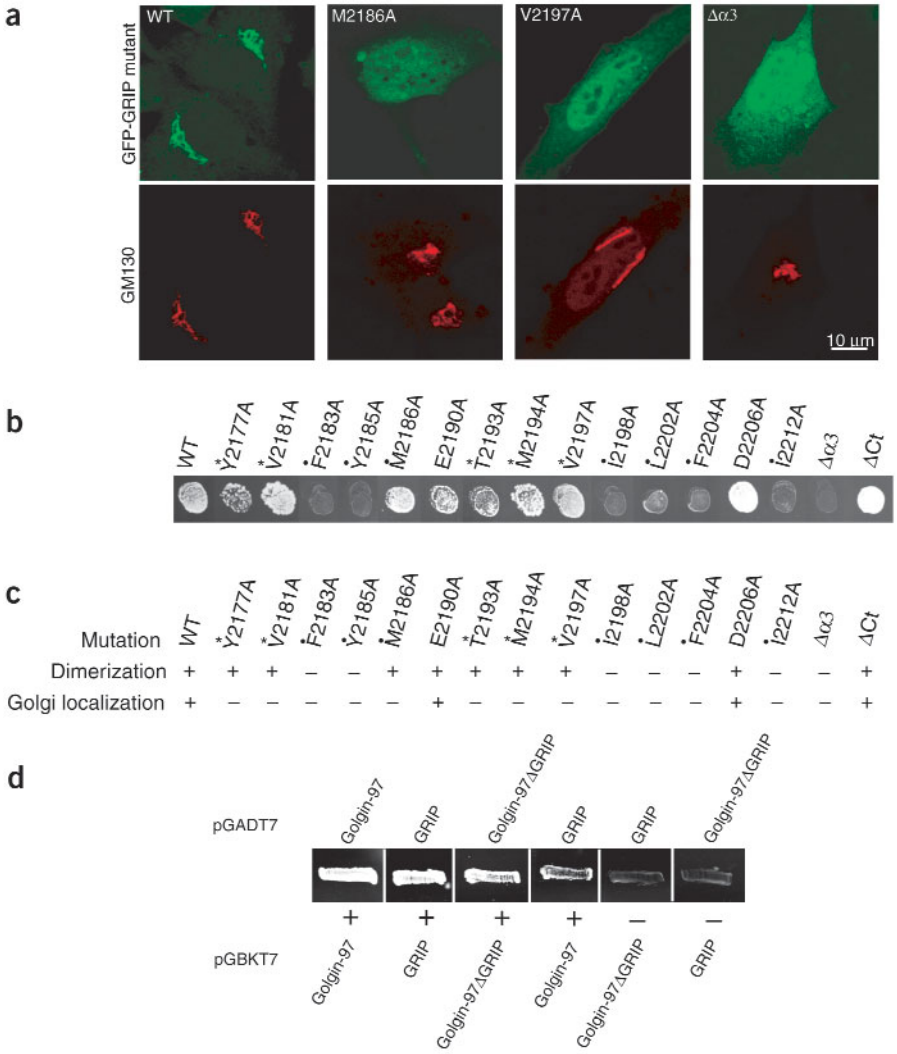

Figure 4 Cellular localization and yeast two-hybrid assays of golgin-245 GRIP domain mutants. (**a**) Cellular localization of representative mutants, including wild type (WT, Golgi), M2186A, V2197A and Δα3. GFP-tagged GRIP mutants and GM130 are in upper and lower panels, respectively. (**b**) Effects of mutations on the GRIP domain dimerization examined by yeast two-hybrid assays. Residues in the Arl1–GRIP interface, *; residues in the GRIP–GRIP interface, •. (**c**) The scores of the dimerization and Golgi distribution of GRIP mutants. Dimerization or Golgi localization, +; no self-interaction or cytosolic distribution, –. E2190A, D2206A and ΔCt mutants serve as negative controls. (**d**) Golgin-97 forms homodimer in a parallel manner through the self-interaction of both its GRIP domain and coiled-coil regions. Plus and minus signs indicate positive and negative interactions, respectively, in yeast two-hybrid assays.

ing the GRIP domain dimerization also abolish its interaction with Arl1-GTP, thus affecting its Golgi localization. Moreover, removal of helix α3 of GRIP domain and the further C-terminal tail (mutant Δα3) abolished the Golgi targeting of golgin-245, whereas truncation of the C-terminal tail alone (mutant ΔCt; residues 2222–2230) had no such effect (**Fig. 4a**,**c**). To test the effects of GRIP mutations on dimer formation, we examined GRIP mutants that have been found to abolish Golgi targeting by yeast two-hybrid assays. F2183A, Y2185A, I2198A, L2202A, F2204A and I2212A mutants and mutant Δα3 (representing truncation of Δα3) abolished the GRIP domain self-interaction, but the M2186 mutant did not. Mutant ΔCt (representing deletion of the C-terminal tail) and mutants targeting residues in the Arl1–GRIP interface, such as Y2177A, V2181A, T2193A, M2194A and V2197A, did not affect GRIP dimerization (**Fig. 4b**,**c**). Although mutant M2186A, unexpectedly, showed self-interaction in yeast two-hybrid assays (**Fig. 4b**,**c**), it did not interact with Arl1-GTP (M.W., L.L., W.G. and H.S., unpublished data) and failed to target the Golgi apparatus (**Fig. 4a**). We propose that the self-interaction of M2186A reflects oligomerization and/or aggregation rather than productive dimerization. Such oligomerization and/or aggregation could not create an interacting surface for Arl1-GTP, thereby leading to defective Golgi targeting. Our preliminary observation that the majority of mutant M2186A is present in the insoluble fraction when expressed in bacteria is consistent with this possibility. Collectively, these results suggest that the integrated GRIP dimer is the structural and functional unit essential for the interaction with Arl1 and thereafter for Golgi targeting.

The observations that GRIP domain forms a parallel homodimer with all three helices involved are independently supported by our yeast two-hybrid studies on golgin-97. Golgin-97 interacts with itself well (**Fig. 4d**). Both the GRIP domain and the coiled-coil region can independently self-interact, suggesting that there are two independent dimerizing interactions, one mediated by the GRIP–GRIP domain interaction and the other mediated by the interaction between the two coiled-coils. Consistent with this, the GRIP domain of golgin-97 did not interact with the coiled-coil region (**Fig. 4d**). These results suggest that golgin-97 (and probably golgin-245) form an extensive parallel dimer in which the dimerized GRIP domains interact with Arl1-GTP to mediate Golgi targeting, thus exposing the extensive coiled-coil region to the cytosol for additional function.

Conformational switch of Arl1 and GRIP binding

Arl1-GTP recruits the GRIP domain to the Golgi membrane, whereas the Arl1-GDP has no such activity[28]. To study the structural basis of the conformational switch upon GTP binding in Arl1 and its effects on GRIP binding, we compared the Arl1 in the complex of Arl1–GRIP with the *Saccharomyces cerevisiae* Arl1 (scArl1) in GDP form[33] (PDB entry 1MOZ), mouse Arl3 (mArl3) in GDP form[34] (PDB entry 1FZQ) and mouse Arl2-GTP (mArl2) in the complex Arl2-GTP–PDEδ[35] (PDB entry 1KSG). All three of these structures are very similar (pairwise r.m.s. deviation of 0.4 Å) with the largest deviations in the switch regions.

As previously observed in the GTP-GDP structural cycles of ARF1 (refs. 36–38) and ARF6 (ref. 39), the switch I region of Arl1 undergoes a marked conformational change upon GDPNP binding (**Fig. 5**). In the GDP forms of scArl1 and mArl3, switch I is folded into an additional β-strand (β_{2E}) that forms part of the central β-sheet and is antiparallel to the β_2 strand[33,34]. The top of the switch I region would extend out and insert between helices α1 and α2 of GRIP domain (**Fig. 5a**,**b**), thus causing severe steric hindrance in the GRIP-binding

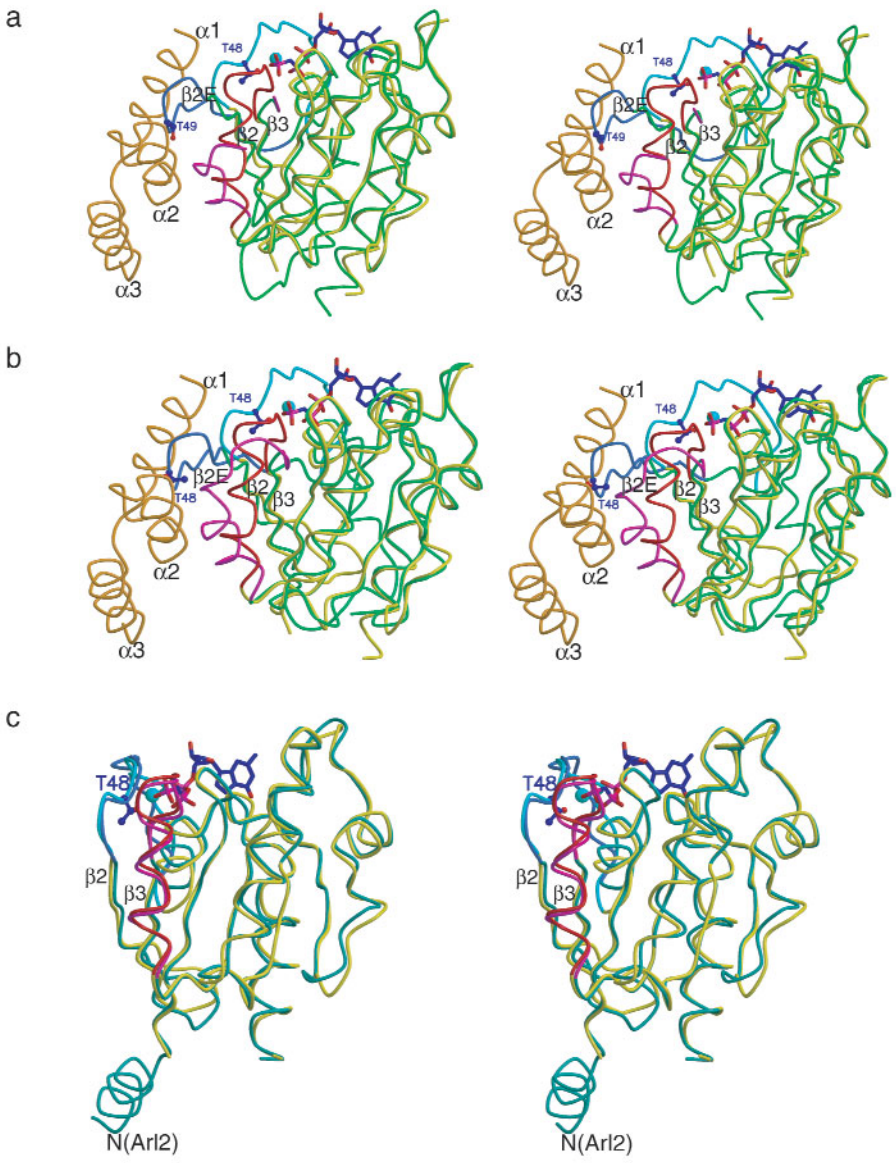

Figure 5 Structural comparisons of Arl1-GTP in the Arl1–GRIP complex with other Arls. (**a**) Stereo view of superposition of Arl1-GTP and *S. cerevesiae* Arl1-GDP (scArl1). The GRIP domain (chain E) is orange, Arl1-GTP molecule (chain A) yellow and scArl1 green. The switch I and II regions in Arl1-GTP are cyan and red, respectively, and those in scArl1 are blue and magenta, respectively. GDPNP and Mg^{2+} from Arl1-GTP are shown in stick model and as cyan sphere, respectively. Residues Thr48 (Arl1-GTP) and Thr49 (scArl1) are shown in ball-and-stick model. (**b**) Stereo view of superposition of Arl1-GTP and mouse Arl3-GDP (mArl3). The coloring scheme is as in **a** except that mArl3 is bright green. Residues Thr48 of both Arl1-GTP and mArl3 are shown as ball-and-stick. (**c**) Stereo view of superposition of Arl1-GTP and mouse Arl2-GTP (mArl2). The coloring scheme is as in **a** except that mArl2 is light green. Only Thr48 of Arl1-GTP is shown as ball-and-stick. The N terminus of mArl2 is labeled.

site on the Arl1 surface groove to prevent GRIP binding. In the GTP state of Arl1, the additional β-strand (β_{2E}) is unfolded, bringing Thr48 close to the nucleotide, where it plays its canonical role in magnesium and γ-phosphate coordination, thus effectively relieving the steric blockage on the GRIP-binding site imposed by the switch I region (**Fig. 5a**,**b**). The conformation of the switch II region, which contributes most of the specificity for GRIP binding (see above), is also changed upon GDPNP binding but to a lesser extent than that of the switch I region. In the GDP form of both scArl1 and mArl3, the upper part of the switch II helix would clash with the helix α2 of GRIP domain and most of the residues that interact with GRIP would not be accessible, thereby preventing them from binding to GRIP (**Fig. 5a**,**b**). In the GTP form of Arl1, the axis of this helix shifted by 15°. As a consequence of this shift, the whole range of switch II moves toward the central β-sheet (**Fig. 5a**,**b**). The conformational change not only enables Gly70 of the DXGGQ motif (residues 67–71) in the switch II region to adopt its canonical role in the coordination of the γ-phosphate, but also allows the binding of the switch II region to the α2 helix of GRIP domain.

The switch regions of Arl1-GTP are essentially the same as those in Arl2-GTP, although they bind different effectors (**Fig. 5c**). In the GTP form of Arl2, the interswitch region (residues 51–67) undergoes a β-sheet register in which β-strands β2 and β3 shift by two residues relative to the remaining β-sheet[35]. Such a considerable conformational change causes the N-terminal region of Arl2 to form an amphipathic helix exposed to the solvent. This helix has been proposed to interact with the membrane as observed with ARF proteins[3,38]. In our crystal structure, the N-terminal 14 residues have been removed to facilitate crystallization. However, because the fold of the Arl1-GTP is markedly similar to that of Arl2-GTP, it is tempting to speculate that the N-terminal region of Arl1 may also fold into a solvent-exposed helix, thereby allowing Arl1 to anchor on the Golgi membrane by myristoylation of Gly2 in the N terminus.

DISCUSSION

Arls belong to the ARF GTPase family, but the two subfamilies have different functions and bind different effectors[6,7]. The ARF1 in GTP form interacts with the GAT domain of GGAs, adaptor proteins with a crucial role in vesicular transport[40–42]. The crystal structure of ARF1-GTP in complex with the N-terminal helix-loop-helix region of GAT domain shows that both the switch and interswitch regions of ARF1 interact with the GAT domain, and the helix-loop-helix motif of GAT domain is positioned directly against the interswitch region of ARF1 (ref. 42; **Fig. 6**). Our crystal structure of the Arl1–GRIP complex shows similar interactions in which the first two helices α1 and α2 (helix-loop-helix) of GRIP interact with both the switch and interswitch regions (**Figs. 2a** and **6**). Moreover, the crystal structure of Arl2-GTP in complex with its effector PDEδ shows that the interactions of Arl2-GTP with PDEδ also involve the switch and interswitch regions[35] (**Fig. 6**). The involvement of the switch I, II and interswitch regions accounts for the specificity of the GTP-bound forms of these small GTPases for their respective effector molecules.

The structure of the Arl1–GRIP domain complex shows why Arl1 but not other ARF or Arl proteins interacts with the GRIP domain of

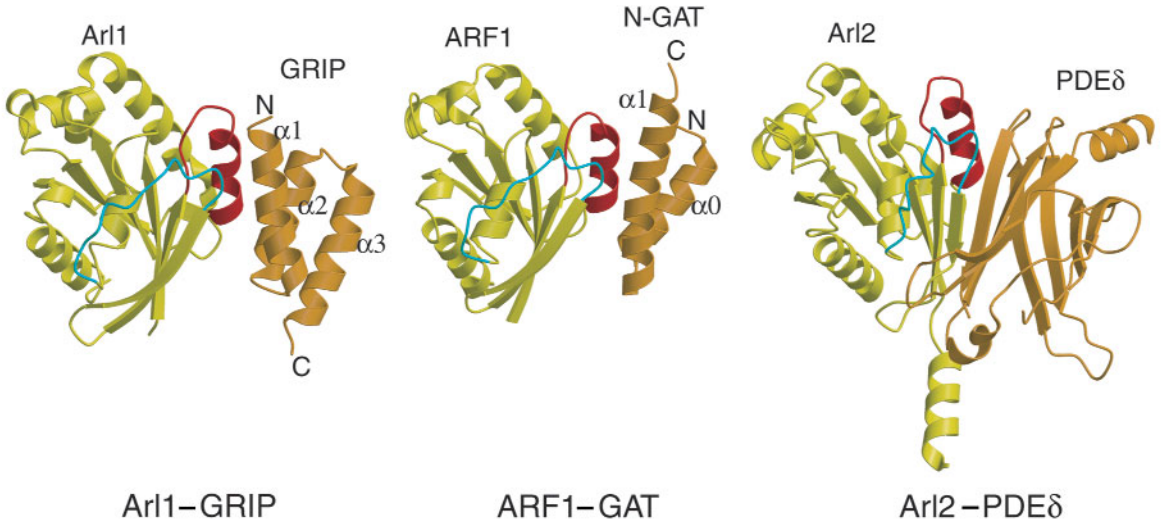

Figure 6 Structural comparisons of the complexes of Arl1–GRIP, ARF1–GAT and Arl2–PDEδ. Arl1, ARF1 and Arl2 are yellow. The effector molecules GRIP, GAT and PDEδ are orange. The switch I and II regions are cyan and red, respectively.

golgin-245. The binding specificity of Arl1-GTP for the GRIP domain is mainly conferred by the residues in the switch II region, with contributions from additional residues in the switch I and interswitch regions. The combined interaction of the residues in the switch II region with GRIP domain validates our earlier mutational studies of the Arl1 switch II region, showing that the collective action of these residues is more important than any individual residue[28]. Because Gln64, Ser73, Tyr77 and Cys80, which are located in the switch II and interswitch regions and are involved in the Arl1–GRIP interface, are specifically present in the Arl1 of diverse species but not in other ARF proteins, the specificity of Arl1 versus that of other ARF proteins for GRIP domain recognition is probably conferred by these four residues. Cys80 is present only in Arl1, whereas this residue is replaced by a polar residue (such as asparagine, serine or histidine) in other Arls. Cys80 is located in the hydrophobic interface in the structure of the Arl1–GRIP complex. Our structural data combined with the earlier mutational studies on this residue suggest this residue confers at least part of the specificity of Arl1 versus other Arls for GRIP domain recognition.

GDP-bound Arl1 has little or no binding activity to the Golgi membrane and is mainly cytosolic[6]. Structural comparison of the GDP- and GTP-bound Arl1 revealed that both the switch I and II regions prevent GRIP binding to Arl1-GDP (see above). The transition of the inactive GDP form to the active GTP form of Arl1 catalyzed by the nucleotide exchange GEF causes marked changes in the conformation of the switch regions, thus effectively relieving the steric hindrance imposed by the switch regions and allowing the high-affinity binding

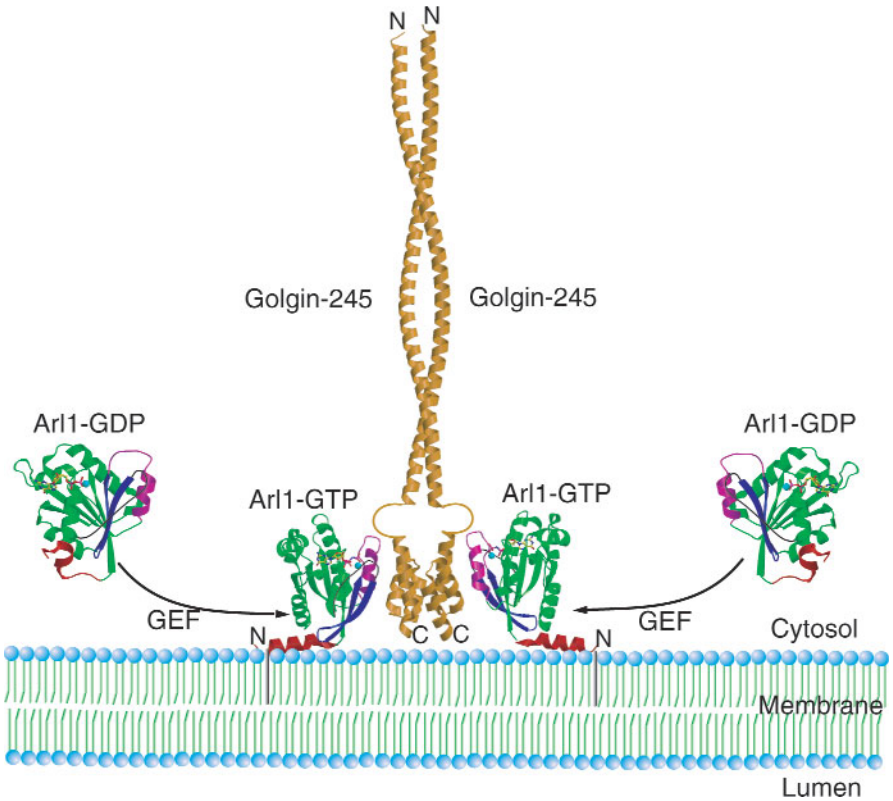

Figure 7 Schematic model of recruitment of Golgin-245 to the Golgi membrane by Arl1. Arl1-GDP is localized to the cytoplasm. Upon the GDP to GTP transition catalyzed by a yet unidentified GEF, Arl1-GTP is localized to Golgi membrane by the anchoring of its myristoylated N terminus to the membrane. The Arl1-GTP could recruit golgin-245 to the Golgi membrane by interacting with its GRIP domain. Golgin-245 forms a parallel dimer in which its coiled-coil region and GRIP domain are independently dimerized. Each subunit of the GRIP dimer interacts separately with one Arl1-GTP molecule, thus efficiently anchoring golgin-245 to the membrane. Switch I, interswitch, switch II regions and the N-terminal region of Arl1 are black, blue, magenta and red respectively. GDP and GTP molecules are shown in stick models and Mg^{2+} as cyan sphere.

Table 1 Data collection and refinement statistics

Data collection	
Space group	*P*1
Unit cell dimensions	
a (Å)	42.08
b (Å)	86.92
c (Å)	86.24
α (°)	118.11
β (°)	99.65
γ (°)	95.47
Resolution range (Å)	39–2.1
Reflections	55,269
Completeness (%)	97.1
R_{merge} (%)[a]	7.5
I / σ	6.7
Refinement	
Total atoms	7,380
Resolution range (Å)	20–2.3
R_{work} (%)[b]	24.5
R_{free} (%)[c]	26.0
R.m.s deviations from ideal values	
Bond length (Å)	0.011
Bond angle (°)	1.7

[a] $R_{merge} = \Sigma_h \Sigma_j |I_j(h) - \langle I(h) \rangle| / \Sigma_h \Sigma_j I_j(h)$, where $I_j(h)$ is the j^{th} measurement of reflection of indices h and $\langle I(h) \rangle$ is the mean intensity. [b] $R_{work} = \Sigma_h ||F_o(h)| - |F_c(h)|| / \Sigma_h |F_o(h)|$, where $F_o(h)$ and $F_c(h)$ are the observed and calculated structure factor amplitudes, respectively, for reflection h calculated against all data included in the refinement. [c] R_{free} is calculated similarly to R_{work} for 5% of randomly chosen reflections not included at any stage in the refinement.

of GRIP domain to Arl1-GTP. Furthermore, the GDP-to-GTP transition of Arl1 also causes the β-sheet register shift in the interswitch region, thereby exposing the myristoylated N terminus to the cytoplasm so that it can bind to the Golgi membrane. In *S. cerevisiae*, Arl3p is required for normal Golgi localization of Arl1p, suggesting that the GEF of Arl1 is regulated by Arl3p and its mammalian homologs ARFRP1 (refs. 29–31).

Our structure shows that Arl1-GTP interacts with the GRIP domain of golgin-245 predominantly in a hydrophobic manner. These interactions suggest that Arl1-GTP recognizes the GRIP domain specifically and directly, with the switch II region providing the main binding affinity. Mutations that abolished the GRIP domain localization have been mapped on the Arl1–GRIP interface, confirming earlier findings that the interaction between Arl1-GTP and GRIP domain is essential for Golgi targeting of GRIP domain golgins[21–23,27]. The GRIP domain folds into an antiparallel array of α-helices that is stabilized only by homodimerization. Mutations of residues involved in the GRIP domain dimerization are expected to destabilize this array and abolish its ability to interact with Arl1-GTP and Golgi targeting. Our mutational studies of Phe2183, Tyr2185, Ile2198, Leu2202, Phe2204 and Ile2212, which are implicated in GRIP domain dimerization, support this conclusion (**Fig. 4b**,**c**).

The crystal structure of GRIP domain in complex with Arl1-GTP shows that the GRIP domain dimer is the structural and functional unit that creates two symmetric surfaces on the two distal sides of the dimer to interact with two separate Arl1-GTP molecules. These two Arl1-GTP molecules seem to anchor the GRIP domain dimer effectively onto the surface of the Golgi membrane. Consistent with the structural interpretation that the dimer of golgin-245 GRIP domain is parallel in nature, we have also shown evidence of two dimerizing regions in golgin-97 by yeast two-hybrid interaction assays. Golgin-97 and golgin-245 are probably parallel homodimers anchored to the Golgi membrane by activated Arl1, which interacts with their GRIP domains. The structure not only mechanistically clarifies the previous mutational studies of GRIP domain and Arl1 but also provides new insight into the molecular basis of Arl1-GTP-mediated Golgi targeting, with support from our additional structure-based mutational studies. As predicted, mutation of several residues implicated in the GRIP dimerization abolished Golgi targeting. Golgi targeting of golgin-245 (and probably golgin-97 and other GRIP domain proteins) involves at least two coupled events (**Fig. 7**). First, golgin-245 forms a parallel dimer mediated by the GRIP domain and probably by the coiled-coil region. The dimerization of GRIP domain creates two symmetric and independent surfaces for interaction with two separate Arl1-GTP molecules, allowing golgin-245 to effectively target the membrane. Such a structurenot only stabilizes the association of golgin-245 with the membrane but also allows the rest of the golgin-245 dimer to be flexible enough to serve additional interactions and functions. Our current structural and mutational studies, in conjunction with the previous results, provide a framework for future studies of golgin-245, golgin-97 and other golgins.

METHODS

Protein expression, purification and crystallization. Both Rat Arl1 (residues 15–181) and human golgin-245 GRIP domain (residues 2171–2230) were cloned into pGEX-6p-1 (Amersham) and expressed as GST-fusion proteins in *Escherichia coli* BL-21 cells. Cells expressing GRIP domain were resuspended in a lysis buffer (20 mM Tris-HCl, pH 7.6, 500 mM NaCl, 2 mM DTT, 1 mM EDTA, 0.1 mM PMSF, 2 mM genzamide and 1 mg ml^{-1} lysozyme) for 30 min, and lysed by sonication. The clarified cell lysate was loaded onto a glutathione-Sepharose 4B column (Amersham). GST-fusion protein was eluted by glutathione and cleaved by PreScission protease (Amersham) overnight at 4 °C. After desalting, cleaved protein was loaded on a glutathione-Sepharose 4B column again and further purified by Superdex 75 (Amersham) gel filtration column chromatography. Eluted golgin-245 GRIP domain was concentrated to 12 mg ml^{-1}. Cells expressing Arl1 were lysed with the above lysis buffer containing 2 mM Mg^{2+} instead of EDTA. Arl1 was purified as GRIP domain described above. After gel filtration, eluted Arl1 was concentrated to 10 mg ml^{-1}. Purified Arl1 was converted to GTP-bound form with GDPNP. In brief, 5 mM EDTA was added to chelate the Mg^{2+} and then the protein was incubated with calf alkaline phosphatase (5 units mg^{-1} protein) and 10 mM GDPNP overnight at 4 °C. Nucleotide exchange was stopped by excess Mg^{2+}. The Arl1 protein solution was mixed with concentrated GRIP domain and incubated on ice for 30 min. The complex of Arl1 and GRIP domain was purified by Superdex 75 gel filtration column chromatography. Eluted complex solution was concentrated to 10 mg ml^{-1}. The identities of Arl1 and GRIP domain were checked by mass spectrometry and N-terminal sequencing.

Crystals of Arl1–GRIP complex were grown in hanging drops by mixing equal amounts of a protein solution (7.5 mg ml^{-1}) and reservoir solution (17–18% (w/v) PEG3350, 200 mM KSCN, 20 mM Tris-HCl, pH 8.0) at 20 °C. Crystals were cryoprotected by transfer to a cryobuffer containing 20% (w/v) PEG3350, 200 mM KSCN, 20 mM Tris-HCl, pH 8.0, 25% (v/v) glycerol and flash-freezing in liquid nitrogen.

Structure determination and refinement. Diffraction data were collected at 100 K on beamline BW7A at Deutsches Elektronen Synchrotron (DESY, Hamburg, Germany). Data were processed using DENZO and intensities were reduced and scaled using SCALEPACK[43]. There are four Arl1 molecules and four GRIP domains in the asymmetric unit of the crystals (**Table 1**).

The crystal structure of Arl1–GRIP was solved using the molecular replacement method with AMoRe[44]. The mouse Arl2-GTP (PDB entry 1KSG) was used as a search model. The model of GRIP domain was automatically built using prime-and-switch mode in RESOLVE[45]. The subsequent model rebuilding was done using O[46]. Refinement was done using CNS[47] and the solvent molecules were included automatically. The final round of the refinement was done with REFMAC5[48] (**Table 1**). The Ramachandran plot shows that 88.7% of residues are in the most favorable region and no residue is in the disallowed region. All figures were produced using MOLSCRIPT[49].

Yeast two-hybrid and cellular localization. Interaction assays of golgin-97 (full length), golgin-97 GRIP and its GRIP domain using the yeast two-hybrid method were done as described[28]. Golgin-245 wild-type GRIP domain (residues 2171–2230) was subjected to standard PCR-mediated mutagenesis to introduce alanine point mutations (Y2172A, V2181A, F2183A, Y2185A, M2186A, E2190A, T2193A, M2194A, V2197A, I2198A, L2202A, F2204A, D2206A or I2212A) or truncation (Δα3 or ΔCt). Δα3 is a truncated version of GRIP domain containing only its α1 and α2 regions (residues 2171–2205). ΔCt consists of the α1, α2 and α3 regions (2171–2222) of GRIP domain, lacking its extreme C terminus. All golgin-245 GRIP mutants and wild type were inserted into pGBKT7, pGADT7 and pEGFP-C2 vectors (BD Clontech). For each mutant, its pGBKT7 and pGADT7 clones were tested for self-interaction (dimerization) in synthetic dropout medium without tryptophan, leucine and histidine and its pEGFP-C2 clone was individually transfected into HeLa cells. After indirect labeling of the Golgi apparatus using GM130 monoclonal antibody (BD Transduction Laboratories), cellular localization of each mutant was examined using a Bio-Rad MRC1024 confocal microscope as described[28].

Coordinates. The coordinates and structure-factor amplitudes of the Arl1–GRIP complex have been deposited in the Protein Data Bank (accession code 1R4A).

ACKNOWLEDGMENTS

We thank P. Tucker at BW7A (European Molecular Biology Laboratory, Hamburg, Germany) for assistance and access to synchrotron radiation facilities, and M.J. Fritzler and E.K.L. Chan for providing the full-length cDNA of human golgin-97. This work is financially supported by the Agency for Science, Technology and Research (A*STAR) in Singapore (to W.H. and H.S.).

COMPETING INTERESTS STATEMENT

The authors declare that they have no competing financial interests.

Received 6 October; accepted 20 November 2003
Published online at http://www.nature.com/natstructmolbiol/

1. Carter, L.L., Redelmeier, T.E., Woollenweber, L.A. & Schmid, S.L. Multiple GTP-binding proteins participate in clathrin-coated vesicle-mediated endocytosis. *J. Cell Biol.* **120**, 37–45 (1993).
2. Schwaninger, R., Plutner, H., Bokoch, G.M. & Balch, W.E. Multiple GTP-binding proteins regulate vesicular transport from the ER to Golgi membranes. *J. Cell Biol.* **119**, 1077–1096 (1992).
3. Boman, A.L. & Kahn, R.A. Arf proteins: the membrane traffic police? *Trends Biochem. Sci.* **20**, 147–150 (1995).
4. Lowe, S.L., Wong, S.H. & Hong, W. The mammalian ARF-like protein 1 (Arl1) is associated with the Golgi complex. *J. Cell Sci.* **109**, 209–220 (1996).
5. Schurmann, A. *et al.* Cloning of two novel ADP-ribosylation factor-like proteins and Characterization of their differential expression in 3T3-L1 cells. *J. Biol. Chem.* **269**, 15683–15688 (1994).
6. Lu, L., Horstmann, H., Ng, C. & Hong, W.J. Regulation of Golgi structure and function by ARF-like protein 1 (Arl1). *J. Cell Sci.* **114**, 4543–4555 (2001).
7. Van Valkenburgh, H., Shern, J.F., Sharer, J.D., Zhu, X. & Kahn, R.A. ADP-ribosylation factors (ARFs) and ARF-like 1 (ARL1) have both specific and shared effectors: characterizing ARL1-binding proteins. *J. Biol. Chem.* **276**, 22826–22837 (2001).
8. Bhamidipati, A., Lewis, S.A. & Cowan, N.J. ADP ribosylation factor-like protein 2 (Arl2) regulates the interaction of tubulin-folding cofactor D with native tubulin. *J. Cell Biol.* **149**, 1087–1096 (2000).
9. Fleming, J.A., Vega, L.R. & Solomon, F. Function of tubulin binding proteins *in vivo*. *Genetics* **156**, 69–80 (2000).
10. Cuvillier, A. *et al.* LdARL-3A, a *Leishmania* promastigote-specific ADP-ribosylation factor-like protein, is essential for flagellum integrity. *J. Cell Sci.* **113**, 2065–2074 (2000).
11. Antoshechkin, I. & Han, M. The *C. elegans* evl-20 gene is a homolog of the small GTPase ARL2 and regulates cytoskeleton dynamics during cytokinesis and morphogenesis. *Dev. Cell* **2**, 579–591 (2002).
12. Tzafrir, I. *et al.* Diversity of TITAN functions in *Arabidopsis* seed development. *Plant Physiol.* **128**, 38–51 (2002).
13. Grayson, C. *et al.* Localization in the human retina of the X-linked retinitis pigmentosa protein RP2, its homologue cofactor C and the RP2 interacting protein Arl3. *Hum. Mol. Genet.* **11**, 3065–3074 (2002).
14. Sharer, J.D. & Kahn, R.A. The ARF-like 2 (ARL2)-binding protein, BART. Purification, cloning, and initial characterization. *J. Biol. Chem.* **274**, 27553–27561 (1999).
15. Ingley, E. *et al.* A novel ADP-ribosylation like factor (ARL-6), interacts with the protein-conducting channel SEC61β subunit. *FEBS Lett.* **459**, 69–74 (1999).
16. Jacobs, S. *et al.* ADP-ribosylation factor (ARF)-like 4, 6, and 7 represent a subgroup of the ARF family characterization by rapid nucleotide exchange and a nuclear localization signal. *FEBS Lett.* **456**, 384–388 (1999).
17. Lin, C.Y. *et al.* ARL4, an ARF-like protein that is developmentally regulated and localized to nuclei and nucleoli. *J. Biol. Chem.* **275**, 37815–37823 (2000).
18. Schurmann, A. *et al.* Reduced sperm count and normal fertility in male mice with targeted disruption of the ADP-ribosylation factor-like 4 (Arl4) gene. *Mol. Cell Biol.* **22**, 2761–2768 (2002).
19. Lin, C.Y., Li, C.C., Huang, P.H. & Lee, F.J. A developmentally regulated ARF-like 5 protein (ARL5), localized to nuclei and nucleoli, interacts with heterochromatin protein 1. *J. Cell Sci.* **115**, 4433–4445 (2002).
20. Buttitta, L., Tanaka, T.S., Chen, A.E., Ko, M.S. & Fan, C.M. Microarray analysis of somitogenesis reveals novel targets of different WNT signaling pathways in the somitic mesoderm. *Dev. Biol.* **258**, 91–104 (2003).
21. Munro, S. & Nichols, B.J. The GRIP domain—a novel Golgi-targeting domain found in several coiled-coil proteins. *Curr. Biol.* **9**, 377–380 (1999).
22. Kjer-Nielsen, L., Teasdale, R.D., van Vliet, C. & Gleeson, P.A. A novel Golgi-localisation domain shared by a class of coiled-coil peripheral membrane proteins. *Curr. Biol.* **9**, 385–388 (1999).
23. Barr, F.A. A novel Rab6-interacting domain defines a family of Golgi-targeted coiled-coil proteins. *Curr. Biol.* **9**, 381–384 (1999).
24. Luke, M.R., Kjer-Nielsen, L., Brown, D.L., Stow, J.L. & Gleeson, P.A. GRIP domain-mediated targeting of two new coiled-coil proteins, GCC88 and GCC185, to subcompartments of the trans-Golgi network. *J. Biol. Chem.* **278**, 4216–4226 (2003).
25. Gillingham, A.K. & Munro, S. Long coiled-coil proteins and membrane traffic. *Biochim. Biophys. Acta* **1641**, 71–85 (2003).
26. Brown, D.L. *et al.* The GRIP domain is a specific targeting sequence for a population of trans-Golgi network derived tubulo-vesicular carriers 1. *Traffic* **2**, 336–344 (2001).
27. Kjer-Nielsen, L., van Vliet, C., Erlich, R., Toh, B.H. & Gleeson, P.A. The Golgi-targeting sequence of the peripheral membrane protein p230. *J. Cell Sci.* **112**, 1645–1654 (1999).
28. Lu, L. & Hong, W. Interaction of Arl1-GTP with GRIP domains recruits auto- antigens Golgin-97 and Golgin-245/p230 onto the Golgi. *Mol. Biol. Cell* **14**, 3767–3781 (2003).
29. Panic, B., Whyte, J.R. & Munro, S. The ARF-like GTPases Arl1p and Arl3p act in a pathway that interacts with vesicle-tethering factors at the Golgi apparatus. *Curr. Biol.* **13**, 405–410 (2003).
30. Setty, S.R., Shin, M.E., Yoshino, A., Marks, M.S. & Burd, C.G. Golgi recruitment of GRIP domain proteins by Arf-like GTPase 1 is regulated by Arf-like GTPase 3. *Curr. Biol.* **13**, 401–404 (2003).
31. Jackson, C.L. Membrane traffic: Arl GTPases get a GRIP on the Golgi. *Curr. Biol.* **13**, R174–176 (2003).
32. Paduch, M., Jelen, F. & Otlewski, J. Structure of small G proteins and their regulators. *Acta Biochim Pol.* **48**, 829–850 (2001).
33. Amor, J.C. *et al.* Structures of yeast ARF2 and ARL1: distinct roles for the N terminus in the structure and function of ARF family GTPases. *J. Biol. Chem.* **276**, 42477–42484 (2001).
34. Hillig, R.C. *et al.* Structural and biochemical properties show ARL3-GDP as a distinct GTP binding protein. *Struct. Fold Des.* **8**, 1239–1245 (2000).
35. Hanzal-Bayer, M., Renault, L., Roversi, P., Wittinghofer, A. & Hillig, R.C. The complex of Arl2-GTP and PDE delta: from structure to function. *EMBO J.* **21**, 2095–2106 (2002).
36. Amor, J.C., Harrison, D.H., Kahn, R.A. & Ringe, D. Structure of the human ADP-ribosylation factor 1 complexed with GDP. *Nature* **372**, 704–708 (1994).
37. Greasley, S.E. *et al.* The structure of rat ADP-ribosylation factor-1 (ARF-1) complexed to GDP determined from two different crystal forms. *Nat. Struct. Biol.* **2**, 797–806 (1995).
38. Goldberg, J. Structural basis for activation of ARF GTPase: mechanisms of guanine nucleotide exchange and GTP-myristoyl switching. *Cell* **95**, 237–248 (1998).
39. Pasqualato, S., Menetrey, J., Franco, M. & Cherfils, J. The structural GDP/GTP cycle of human Arf6. *EMBO Rep.* **2**, 234–238 (2001).
40. Collins, B.M., Watson, P.J. & Owen, D.J. The structure of the GGA1-GAT domain reveals the molecular basis for ARF binding and membrane association of GGAs. *Dev. Cell* **4**, 321–432 (2003).
41. Suer, S., Misra, S., Saidi, L.F. & Hurley, J.H. Structure of the GAT domain of human GGA1: a syntaxin amino-terminal domain fold in an endosomal trafficking adaptor. *Proc. Natl. Acad. Sci.* **100**, 4451–4456 (2003).
42. Shiba, T. *et al.* Molecular mechanism of membrane recruitment of GGA by ARF in lysosomal protein transport. *Nat. Struct. Biol.* **10**, 386–393 (2003).
43. Otwinowski, Z. In *Data Collection and Processing* (eds. Sawyer, N.I.L. & Bailey, S.) 56–62 (SERC Daresbury Laboratory, Warrington, UK, 1993).
44. Navaza, J. & Saludjian, P. AMoRe: an automated molecular replacement program package. *Methods Enzymol.* **276**, 581–594 (1997).
45. Terwilliger, T.C. Maximum-likelihood density modification. *Acta Crystallogr. D* **56**, 965–972 (2000).
46. Jones, T.A. & Kjeldgaard, M. Electron-density map interpretation. *Methods Enzymol.* **277**, 173–208 (1997).
47. Brünger, A.T. *et al.* Crystallography & NMR system: a new software suite for macromolecular structure determination. *Acta Crystallogr. D* **54**, 905–921 (1998).
48. Murshudov, G.N, Vagin, A.A. & Dodson, E.J. Refinement of macromolecular structures by the maximum-likelihood method. *Acta Crystallogr. D* **53**, 240–255 (1997).
49. Kraulis, P. J. MOLSCRIPT: a program to produce both detailed and schematic plots of protein structures. *J. Appl. Crystallogr.* **24**, 946–950 (1991).
50. Gouet, P. & Courcelle, E. ENDscript: a workflow to display sequence and structure information. *Bioinformatics* **18**, 767–768 (2002).